Part VI

Other Symmetries

16

Time Reversal Symmetry

In this chapter we consider the properties of the time reversal operator (Sects. 16.1 and 16.2) and the topic of time reversal symmetry. We then consider the effect of time reversal symmetry on the form of the electronic dispersion relations and this topic is discussed here for the case of no spin (Sect. 16.3) and when the spin–orbit interaction is included (Sect. 16.4). As a second illustration of time reversal symmetry, we consider magnetic space groups in Sect. 16.5, where the time reversal operator itself can become a symmetry element of the group.

In high energy physics, arguments regarding time inversion were essential in providing guidance for the development of a theory for the fundamental particles. The CPT invariance in particle physics deals with charge conjugation (C) which is the reversal of the sign of the electrical charge, parity (P) which is spatial inversion, and time inversion (T).

16.1 The Time Reversal Operator

Knowledge of the state of a system at any instant of time t and the deterministic laws of physics are sufficient to determine the state of the system both into the future and into the past. If the wave function $\psi(\boldsymbol{r}, t)$ specifies the time evolution of state $\psi(\boldsymbol{r}, 0)$, then $\psi(\boldsymbol{r}, -t)$ is called the *time-reversed conjugate* of $\psi(\boldsymbol{r}, t)$. The time-reversed conjugate state is achieved by running the system backwards in time or reversing all the velocities (or momenta) of the system.

The time evolution of a state is governed by Schrödinger's equation (one of the deterministic laws of physics)

$$\mathrm{i}\hbar \frac{\partial \psi}{\partial t} = \mathcal{H}\psi \,, \tag{16.1}$$

which is satisfied by a time-dependent wave function of the form

$$\psi(\boldsymbol{r}, t) = e^{\frac{-\mathrm{i}\mathcal{H}t}{\hbar}} \psi(\boldsymbol{r}, 0) \,, \tag{16.2}$$

where $\exp[-\mathrm{i}\mathcal{H}t/\hbar]$ is the time evolution factor. The effect of time reversal $t \to -t$ (which we denote by the operator $\hat{T}$) on the wave function is that of complex conjugation $\psi \to \psi^*$ so that

$$\hat{T}\psi(\boldsymbol{r}, t) = \psi(\boldsymbol{r}, -t) = \psi^*(\boldsymbol{r}, t)\,. \tag{16.3}$$

In Sect. 16.2, we discuss some of the important properties of $\hat{T}$.

16.2 Properties of the Time Reversal Operator

The important properties of the time reversal operator $\hat{T}$ include:

(a) *Commutation*: $[\hat{T}, \mathcal{H}] = 0$
Because of *energy conservation*, the time reversal operator $\hat{T}$ commutes with the Hamiltonian $\hat{T}\mathcal{H} = \mathcal{H}\hat{T}$. Since $\hat{T}$ commutes with the Hamiltonian, eigenstates of the time reversal operator are also eigenstates of the Hamiltonian.

(b) *Antilinear*: $\hat{T}i = -i$
From Schrödinger's equation (16.1), it is seen that the reversal of time corresponds to a change of $i \to -i$, which implies that $\hat{T}i = -i$. We call an operator *antilinear* if its operation on a complex number yields the complex conjugate of the number $\hat{T}a = a^*$ rather than the number itself.

(c) *Complex conjugation of wave functions*:
Since $\hat{T}$ is an antilinear operator, we have $\hat{T}\psi = \psi^*$. Since $\hat{T}\psi = \psi^*$, the action of $\hat{T}$ on a scalar product is

$$\hat{T}(\psi, \phi) = \int \phi^*(\boldsymbol{r})\psi(\boldsymbol{r})d^3r = (\psi, \phi)^*\,. \tag{16.4}$$

(d) In the case of no spin, we have $\hat{T} = \hat{K}$ where $\hat{K}$ is the complex conjugation operator. With spin, we show below that $\hat{T} = \hat{K}\sigma_y$ where σ_y is the Pauli spin operator,

$$\sigma_y = \begin{pmatrix} 0 & -i \\ i & 0 \end{pmatrix}\,.$$

We will see below that both $\hat{T}$ and $\hat{K}$ are antiunitary operators. From Schrödinger's equation (no spin), the effect of $\hat{T}$ on $\boldsymbol{p}$ is to reverse $\boldsymbol{p}$ (time goes backward) and $\hat{T}$ leaves $V(\boldsymbol{r})$ invariant, so that indeed $\mathcal{H}$ is invariant under $\hat{T}$. When spin is included, however, the Hamiltonian $\mathcal{H}$ must still be invariant under $\hat{T}$. We note that $\hat{T}\boldsymbol{p} = -\boldsymbol{p}$ and $\hat{T}\boldsymbol{L} = -\boldsymbol{L}$ (orbital angular momentum). We likewise require that $\hat{T}\boldsymbol{S} = -\boldsymbol{S}$ where $\boldsymbol{S}$ = spin angular momentum. If these requirements are imposed, we show below that the $\mathcal{H}$ is still invariant under $\hat{T}$, that is $\mathcal{H}$ commutes with $\hat{T}$ when the spin–orbit interaction is included:

$$\mathcal{H} = \frac{p^2}{2m} + V(\boldsymbol{r}) + \frac{\hbar}{4m^2c^2}\boldsymbol{\sigma} \cdot (\boldsymbol{\nabla} V \times \boldsymbol{p}) \,. \tag{16.5}$$

To show that $\hat{T}$ commutes with $\mathcal{H}$ when the spin–orbit interaction is included, we first note that $\hat{K}[\sigma_x, \sigma_y, \sigma_z] = [\sigma_x, -\sigma_y, \sigma_z]$ when the spin components are written in terms of the Pauli matrices

$$\begin{aligned} \sigma_x &= \begin{pmatrix} 0 & 1 \\ 1 & 0 \end{pmatrix} , \\ \sigma_y &= \begin{pmatrix} 0 & -i \\ i & 0 \end{pmatrix} , \\ \sigma_z &= \begin{pmatrix} 1 & 0 \\ 0 & -1 \end{pmatrix} , \end{aligned} \tag{16.6}$$

since only the Pauli matrix σ_y contains i. Thus $\hat{K}$ by itself is not sufficient to describe the time reversal operation on the Hamiltonian $\mathcal{H}$ (16.5) when the spin–orbit interaction is included. We will however see below that the product $\hat{K}\sigma_y$ can describe the time reversal of $\mathcal{H}$.
Let us now consider the effect of $\hat{K}\sigma_y$ on the spin matrices $\hat{K}\sigma_y[\sigma_x, \sigma_y, \sigma_z]$. We note that

$$\begin{aligned} \sigma_y\sigma_x = -\sigma_x\sigma_y \quad &\text{so that} \quad \hat{K}\sigma_y\sigma_x = -\hat{K}\sigma_x\sigma_y = -\sigma_x\hat{K}\sigma_y \\ \sigma_y\sigma_z = -\sigma_z\sigma_y \quad &\text{so that} \quad \hat{K}\sigma_y\sigma_z = -\hat{K}\sigma_z\sigma_y = -\sigma_z\hat{K}\sigma_y \,. \end{aligned}$$

Also we have $\hat{K}\sigma_y\sigma_y = -\sigma_y\hat{K}\sigma_y$ since, from above $\hat{K}\sigma_y = -\sigma_y\hat{K}$. Thus we obtain

$$\hat{K}\sigma_y\boldsymbol{\sigma} = -\boldsymbol{\sigma}\hat{K}\sigma_y \,,$$

so that the operator $\hat{K}\sigma_y$ transforms $\boldsymbol{\sigma}$ (or $\boldsymbol{S}$) into $-\boldsymbol{\sigma}$ (or $-\boldsymbol{S}$). Clearly σ_y does not act on any of the other terms in the Hamiltonian.
Since $\hat{K}\hat{K} = \hat{K}^2 = \hat{1}$, where $\hat{1}$ is the unit matrix, we can write the important relation $\hat{T} = \hat{K}\sigma_y$ which implies $\hat{K}\hat{T} = \sigma_y =$ *unitary operator* since $\sigma_y^\dagger\sigma_y^{-1} = \hat{1}$. But also $\sigma_y^2 = \sigma_y\sigma_y = \hat{1}$ so we have $\sigma_y^\dagger = \sigma_y$ and $\sigma_y^{\dagger 2} = \hat{1}$, where the symbol † is used to denote the adjoint of an operator.

(e) In the case of no spin $\hat{T}^2 = \hat{1}$, since $\hat{K}^2 = \hat{1}$ and $\hat{T} = \hat{K}$. With spin we will now show that $\hat{T}^2 = -\hat{1}$. Since $\hat{T} = \hat{K}\sigma_y$ when the effect of the electron spin is included, then

$$\hat{T}^2 = (\hat{K}\sigma_y)(\hat{K}\sigma_y) = -(\sigma_y\hat{K})(\hat{K}\sigma_y) = -\sigma_y\hat{K}^2\sigma_y = -\sigma_y\sigma_y = -\hat{1} \,.$$

More generally if we write $\hat{K}\hat{T} = \hat{U} =$ unitary operator (not necessarily σ_y), we can then show that $\hat{T}^2 = \pm\hat{1}$. Since two consecutive operations by $\hat{T}$ on a state ψ must produce the same physical state ψ, we have $\hat{T}^2 = C\hat{1}$

where C is a phase factor $e^{i\phi}$ of unit magnitude. Since $\hat{K}^2 = \hat{1}$, we can write

$$\hat{K}^2\hat{T} = \hat{T} = \hat{K}\hat{U} = \hat{U}^*\hat{K}\,, \tag{16.7}$$

$$\hat{T}^2 = \hat{K}\hat{U}\hat{K}\hat{U} = \hat{U}^*\hat{K}^2\hat{U} = \hat{U}^*\hat{U} = C\hat{1}\,. \tag{16.8}$$

We show below that $C = \pm\hat{1}$. Making use of the unitary property $\hat{U}^\dagger\hat{U} = \hat{U}\hat{U}^\dagger = \hat{1}$, we obtain by writing $\hat{U}^* = \hat{U}^*\hat{U}\hat{U}^\dagger = C\hat{U}^\dagger$,

$$\hat{U}^* = C\hat{U}^\dagger = C\tilde{U}^*\,, \tag{16.9}$$

where $\tilde{U}$ denotes the transpose of $\hat{U}$. Taking the transpose of both sides of (16.9) yields

$$\tilde{U}^* = \hat{U}^\dagger = C\hat{U}^* = C(C\tilde{U}^*) = C^2\hat{U}^\dagger \quad \text{or} \quad C^2 = 1 \quad \text{and} \quad C = \pm 1\,. \tag{16.10}$$

We thus obtain either $\hat{T}^2 = +\hat{1}$ or $\hat{T}^2 = -\hat{1}$.

(f) Operators $H, \boldsymbol{r}, V(\boldsymbol{r})$ are even under time reversal $\hat{T}$; operators $\boldsymbol{p}, \boldsymbol{L}, \boldsymbol{\sigma}$ are odd under $\hat{T}$. Operators are either even or odd under time reversal. We can think of spin angular momentum classically as due to a current loop in a plane $\perp$ to the z-axis. Time reversal causes the current to flow in the opposite direction.

(g) $\hat{T}$ and $\hat{K}$ are antiunitary operators , as shown below.

In this subsection we show that $\hat{T}$ and $\hat{K}$ are antiunitary operators which means $\hat{T}\hat{T}^\dagger = -\hat{1}$ and $\hat{K}\hat{K}^\dagger = -\hat{1}$. We show below that $\hat{T}$ and $\hat{K}$ are antiunitary whether or not the spin is considered explicitly. The properties of the inverse of $\hat{T}$ and $\hat{K}$ are readily found. Since $\hat{K}^2 = \hat{1}$, then $\hat{K}\hat{K} = \hat{1}$ and $\hat{K}^{-1} = \hat{K}$. If for the case where the spin is treated explicitly $\hat{T}^2 = -\hat{1}$, then $\hat{T}\hat{T} = -\hat{1}$ and $\hat{T}^{-1} = -\hat{T}$; $\hat{T} = \hat{K}\sigma_y$ for the case of spin. For the spinless case, $\hat{T}^2 = \hat{1}$ and $\hat{T}^{-1} = \hat{T}$. Since complex conjugation changes $i \to -i$, we can write $\hat{K}^\dagger = -\hat{K}$ so that $\hat{K}$ is antiunitary.

We now use this result to show that both $\hat{T}$ and $\hat{K}$ are *antiunitary*. This is the most important property of $\hat{T}$ from the point of view of group theory. Since $\hat{K} = \hat{T}$ in the absence of spin, and since $\hat{K}$ is antiunitary, it follows that $\hat{T}$ is antiunitary in this case. However, when spin is included, $\hat{T} = \hat{K}\sigma_y$ and

$$\begin{aligned} \sigma_y &= \hat{K}\hat{T} \\ \sigma_y^\dagger &= \hat{T}^\dagger\hat{K}^\dagger\,. \end{aligned} \tag{16.11}$$

Since σ_y is a unitary operator, thus $\hat{T}^\dagger\hat{K}^\dagger\hat{K}\hat{T} = \hat{1}$ but since $\hat{K}^\dagger\hat{K} = -\hat{1}$ it follows that $\hat{T}^\dagger\hat{T} = -\hat{1}$, showing that $\hat{T}$ is also *antiunitary*.

Furthermore $\hat{K}$ and $\hat{T}$ behave differently from all the operators that we have thus far encountered in group theory, such as the point group operations (rotations, improper rotations, mirror planes, inversion and $\mathcal{R}$ = rotation of

2π must be considered for spin dependent Hamiltonians). Thus in considering symmetry operations in group theory, we treat all the unitary operators separately by use of character tables and all the associated apparatus, and then we treat *time reversal symmetry* as an *additional symmetry constraint*. We will see in Sect. 16.5 how time reversal symmetry enters directly as a symmetry element for magnetic point groups.

We discuss first in Sects. 16.3 and 16.4 the general effect of $\hat{T}$ on the form of $E(\boldsymbol{k})$ for the case of electronic bands neglecting spin (Sect. 16.3) and including spin (Sect. 16.4). In these sections we also consider the question of degeneracies imposed on energy levels by time reversal symmetry (the Herring Rules) [39].

16.3 The Effect of $\hat{T}$ on $E(k)$, Neglecting Spin

If for the moment we neglect spin, then the time reversal operation acting on a solution of Schrödinger's equation yields

$$\hat{T}\psi(\boldsymbol{r}) = \psi^*(\boldsymbol{r})\,. \tag{16.12}$$

Since the Hamiltonian commutes with $\hat{T}$, then both $\psi(\boldsymbol{r})$ and $\psi^*(\boldsymbol{r})$ satisfy Schrödinger's equation for the same energy eigenvalue, so that a twofold degeneracy occurs. We will now show that time reversal symmetry leads to two symmetry properties for the energy eigenvalues for Bloch states: the evenness of the energy eigenvalues $E(\boldsymbol{k}) = E(-\boldsymbol{k})$, and the zero slope of $E_n(\boldsymbol{k})$ at the Brillouin zone boundaries.

The effect of the translation operation on a Bloch state is

$$\psi_k(\boldsymbol{r} + \boldsymbol{R}_n) = \mathrm{e}^{\mathrm{i}\boldsymbol{k}\cdot\boldsymbol{R}_n}\psi_k(\boldsymbol{r})\,, \tag{16.13}$$

and the effect of time reversal is

$$\hat{T}\psi_k(\boldsymbol{r}) = \psi_k^*(\boldsymbol{r})\,. \tag{16.14}$$

We can write the following relation for the complex conjugate of Bloch's theorem

$$\psi_k^*(\boldsymbol{r} + \boldsymbol{R}_n) = \mathrm{e}^{-\mathrm{i}\boldsymbol{k}\cdot\boldsymbol{R}_n}\psi_k^*(\boldsymbol{r})\,, \tag{16.15}$$

and we can also rewrite (16.15) in terms of $\boldsymbol{k} \to -\boldsymbol{k}$ as

$$\psi_{-k}^*(\boldsymbol{r} + \boldsymbol{R}_n) = \mathrm{e}^{\mathrm{i}\boldsymbol{k}\cdot\boldsymbol{R}_n}\psi_{-k}^*(\boldsymbol{r})\,, \tag{16.16}$$

which upon comparing (16.13), (16.15) and (16.16) implies that for nondegenerate levels the time reversal operator transforms $\boldsymbol{k} \to -\boldsymbol{k}$

$$\hat{T}\psi_k(\boldsymbol{r}) = \psi_{-k}(\boldsymbol{r}) = \psi_k^*(\boldsymbol{r})\,. \tag{16.17}$$

If the level is doubly degenerate and $\psi_k(\boldsymbol{r})$ and $\phi_k(\boldsymbol{r})$ are the corresponding eigenstates, then if $\hat{T}\psi_k(\boldsymbol{r}) = \phi_k(\boldsymbol{r}) = \psi_{-k}(\boldsymbol{r})$, and no additional degeneracy

is required by time reversal symmetry. Time reversal symmetry thus implies that for a spinless system

$$E_n(\boldsymbol{k}) = E_n(-\boldsymbol{k})\,, \tag{16.18}$$

and the energy is an even function of wave vector $\boldsymbol{k}$ whether or not there is spatial inversion symmetry.

Using this result (16.18) and the $E(\boldsymbol{k}) = E(\boldsymbol{k}+\boldsymbol{K})$ periodicity in $\boldsymbol{k}$ space, where $\boldsymbol{K}$ is a reciprocal lattice vector, we obtain

$$E\left(\frac{\boldsymbol{K}}{2} - \delta\boldsymbol{k}\right) = E\left(-\frac{\boldsymbol{K}}{2} + \delta\boldsymbol{k}\right) = E\left(\frac{\boldsymbol{K}}{2} + \delta\boldsymbol{k}\right)\,, \tag{16.19}$$

where $\delta\boldsymbol{k}$ is an infinitesimal distance to the Brillouin zone boundary. Thus referring to Fig. 16.1, $E(\boldsymbol{k})$ comes into the zone boundary with *zero slope* for both the lower and upper branches of the solutions in Fig. 16.1. For the case where the energy band shows a degeneracy at the zone boundary, the upper and lower bands will have *equal and opposite slopes*.

We have been using the symmetry properties in (16.18) and (16.19) throughout our solid state physics courses. In the most familiar cases, $E(\boldsymbol{k})$ depends on k^2. Figure 16.1 illustrates the symmetry properties of (16.18) and (16.19) for a simple parabolic band at $\boldsymbol{k} = 0$ and at the Brillouin zone boundary.

Let us now consider the consequences of these ideas from a group theoretical point of view, and enumerate Herring's rules which summarize the effect of time reversal $\hat{T}$ on the irreducible representations of a group. If $\psi(\boldsymbol{r})$ belongs to the irreducible representation D, then $\hat{T}\psi(\boldsymbol{r}) = \psi^*(r)$ will transform according to D^* which consists of the complex conjugate of all the matrices in D. We can distinguish three different possibilities in the case of *no spin*:

(a) All of the matrices in the representation D are real matrices or can be made into real matrices by a unitary transformation. In this case, the time reversal operator leaves the representation D invariant and no additional degeneracies in $E(\boldsymbol{k})$ result.
(b) If the representations D and D^* cannot be brought into equivalence by a unitary transformation, there is a doubling of the degeneracy of such levels due to time reversal symmetry. Then the representations D and D^* are said to form a *time reversal symmetry pair* and these levels will stick together.
(c) If the representations D and D^* can be made equivalent under a suitable unitary transformation, but the matrices in this representation cannot be made real, then the time reversal symmetry also requires a doubling of the degeneracy of D and the bands will stick together.

To illustrate these possibilities, consider the point group C_4 (see Table 16.1). Here irreducible representations A and B are of type (a) above and each of

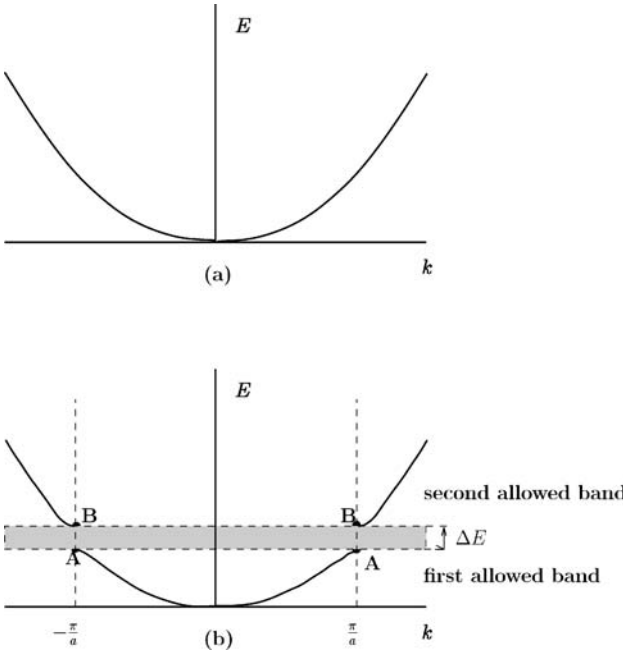

Fig. 16.1. Simple $E(\boldsymbol{k})$ diagram for a spinless electron illustrating both $E(\boldsymbol{k}) = E(-\boldsymbol{k})$ and the zero slope of $E(\boldsymbol{k})$ at the Brillouin zone boundary

Table 16.1. Character table for point group C_4

	C_4 (4)			E	C_2	C_4	C_4^3	time reversal
x^2+y^2, z^2	R_z, z		A	1	1	1	1	(a)
x^2-y^2, xy			B	1	1	-1	-1	(a)
(xz, yz)	(x, y)	}	E	1	-1	i	$-i$	(b)
	(R_x, R_y)	}		1	-1	$-i$	i	(b)

these representations correspond to nondegenerate energy levels. However, the two representations labeled E are complex conjugates of each other and are of type (b) since there is no unitary transformation that can bring them into equivalence. Thus because of the time reversal symmetry requirement, representation E corresponds to a doubly degenerate level. This illustrates the case where time reversal symmetry gives rise to an additional level degeneracy.

The time reversal partners are treated as different representations when applying the following rules on character:

(a) The number of irreducible representations is equal to the number of classes.
(b) $\sum_i \ell_i^2 = h$.

Using the character table for the group of the wave vector, we can distinguish which of the three cases apply for a given irreducible representation using the Herring test [39], which is now discussed. Let Q_0 be an element in the space group which transforms $\boldsymbol{k}$ into $-\boldsymbol{k}$. Then Q_0^2 is an element in the group of the wave vector $\boldsymbol{k}$, since all elements in the group of the wave vector leave k invariant and therefore each of these group elements are elements with the properties of Q_0^2. If the inversion operator i is contained in the group of the wave vector $\boldsymbol{k}$, then all the elements Q_0 are in the group of the wave vector $\boldsymbol{k}$. If i is not an element of the group of the wave vector $\boldsymbol{k}$, then the elements Q_0 may or may not be an element in the group of the wave vector. Let h_{Q_0} equal the number of elements Q_0. The Herring space group test is then

$$\begin{aligned}\sum_R \chi(Q_0^2) &= h_{Q_0} \quad \text{case (a)} \\ &= 0 \quad \text{case (b)} \\ &= -h_{Q_0} \quad \text{case (c)}\,,\end{aligned}$$

where χ is the character for a representation of the group of the wave vector $\boldsymbol{k}$ and the sum is over all the elements of the group. These tests can be used to decide whether or not time reversal symmetry introduces any additional degeneracies to this representation. Information on the Herring test is normally presented in each of the 32 point groups in the character tables in Koster's book [47, 48].

To apply the Herring test to the point group C_4, and consider the group of the wave vector for $\boldsymbol{k} = 0$. Then all four symmetry operations take $\boldsymbol{k} \to -\boldsymbol{k}$ since $\boldsymbol{k} = 0$. Furthermore, $E^2 = E, C_2^2 = E, C_4^2 = C_2$ and $(C_4^3)^2 = C_2$ so that for representations A and B

$$\sum_R \chi(Q_0^2) = 1 + 1 + 1 + 1 = 4 \tag{16.20}$$

from which we conclude that A and B correspond to case (a), in agreement with Koster's tables. On the other hand, for each representation under E,

$$\sum_R \chi(Q_0^2) = 1 + 1 + (-1) + (-1) = 0 \tag{16.21}$$

from which we conclude that representations E correspond to case (b). Therefore the two irreducible representations under E correspond to the same energy and the corresponding $E(\boldsymbol{k})$ will stick together. The two representations under E are called *time reversal conjugate representations.*

16.4 The Effect of $\hat{\boldsymbol{T}}$ on $\boldsymbol{E(k)}$, Including the Spin–Orbit Interaction

When the *spin–orbit interaction is included*, then the Bloch functions transform as irreducible representations of the double group. The degeneracy of the energy levels is different from the spinless situation, and in particular every level is at least doubly degenerate.

When the spin–orbit interaction is included, $\hat{T} = \hat{K}\sigma_y$ and not only do we have $\boldsymbol{k} \to -\boldsymbol{k}$, but we also have $\boldsymbol{\sigma} \to -\boldsymbol{\sigma}$ under time reversal symmetry. This is written schematically as

$$\hat{T}\psi_{n,k\uparrow}(\boldsymbol{r}) = \psi_{n,-k\downarrow}(\boldsymbol{r})\,, \tag{16.22}$$

so that the time reversal conjugate states are

$$E_{n\uparrow}(\boldsymbol{k}) = E_{n\downarrow}(-\boldsymbol{k}) \tag{16.23}$$

and

$$E_{n\downarrow}(\boldsymbol{k}) = E_{n\uparrow}(-\boldsymbol{k})\,. \tag{16.24}$$

If inversion symmetry exists as well,

$$E_n(\boldsymbol{k}) = E_n(-\boldsymbol{k})\,, \tag{16.25}$$

then

$$E_{n\uparrow}(\boldsymbol{k}) = E_{n\uparrow}(-\boldsymbol{k}) \quad \text{and} \quad E_{n\downarrow}(\boldsymbol{k}) = E_{n\downarrow}(-\boldsymbol{k}) \tag{16.26}$$

making $E_{n\uparrow}(\boldsymbol{k})$ and $E_{n\downarrow}(\boldsymbol{k})$ degenerate. In more detail, since $\hat{T} = \hat{K}\sigma_y$ and since

$$\sigma_y \uparrow = \begin{pmatrix} 0 & -i \\ i & 0 \end{pmatrix} \begin{pmatrix} 1 \\ 0 \end{pmatrix} = i \begin{pmatrix} 0 \\ 1 \end{pmatrix} = i \downarrow$$

$$\sigma_y \downarrow = \begin{pmatrix} 0 & -i \\ i & 0 \end{pmatrix} \begin{pmatrix} 0 \\ 1 \end{pmatrix} = -i \begin{pmatrix} 1 \\ 0 \end{pmatrix} = -i \uparrow,$$

we obtain

$$\begin{aligned} \hat{T}\psi_{n,k\uparrow}(\boldsymbol{r}) = \hat{T}\mathrm{e}^{\mathrm{i}\boldsymbol{k}\cdot\boldsymbol{r}} \left[u_{n,k\uparrow} \begin{pmatrix} 1 \\ 0 \end{pmatrix} \right] &= \mathrm{e}^{-\mathrm{i}\boldsymbol{k}\cdot\boldsymbol{r}} \left[i u^*_{n,k\uparrow} \begin{pmatrix} 0 \\ 1 \end{pmatrix} \right] \\ &= \mathrm{e}^{-\mathrm{i}\boldsymbol{k}\cdot\boldsymbol{r}} u_{n,-k\downarrow} \begin{pmatrix} 0 \\ 1 \end{pmatrix}, \end{aligned} \tag{16.27}$$

which is a Bloch state for wave vector $-\boldsymbol{k}$ and spin $\downarrow$. Likewise

$$\begin{aligned} \hat{T}\psi_{n,k\downarrow}(\boldsymbol{r}) = \hat{T}\mathrm{e}^{\mathrm{i}\boldsymbol{k}\cdot\boldsymbol{r}} \left[u_{n,k\downarrow} \begin{pmatrix} 0 \\ 1 \end{pmatrix} \right] &= \mathrm{e}^{-\mathrm{i}\boldsymbol{k}\cdot\boldsymbol{r}} \left[-i u^*_{n,k\downarrow} \begin{pmatrix} 1 \\ 0 \end{pmatrix} \right] \\ &= \mathrm{e}^{-\mathrm{i}\boldsymbol{k}\cdot\boldsymbol{r}} u_{n,-k\uparrow} \begin{pmatrix} 1 \\ 0 \end{pmatrix} \end{aligned} \tag{16.28}$$

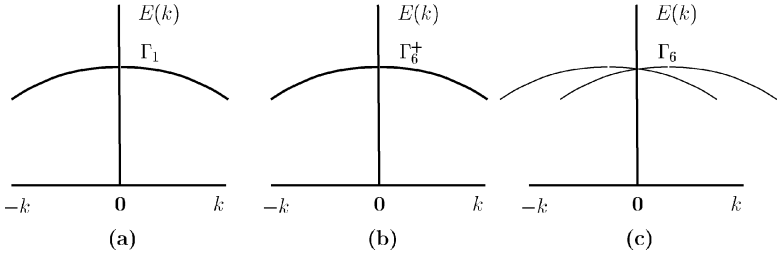

Fig. 16.2. Schematic example of Kramers degeneracy in a crystal in the case of: (**a**) no spin–orbit interaction where each level is doubly degenerate ($\uparrow, \downarrow$), (**b**) both spin–orbit interaction and inversion symmetry are present and the levels are doubly degenerate, (**c**) spin–orbit interaction and no spatial inversion symmetry where the relations (16.23) and (16.24) apply

which is a Bloch state for wave vector $-\boldsymbol{k}$ and spin $\uparrow$ in which we have written

$$iu^*_{n,k\uparrow} = u_{n,-k\downarrow}$$

and

$$-iu^*_{n,k\downarrow} = u_{n,-k\uparrow}\,.$$

For a general point in the Brillouin zone, and in the absence of spin–orbit coupling, but including the spin on the electron, the energy levels have a *necessary twofold spin degeneracy* and also exhibit the property $E(\boldsymbol{k}) = E(-\boldsymbol{k})$, whether or not there is inversion symmetry. This is illustrated in Fig. 16.2(a). When the spin–orbit interaction is turned on and there is inversion symmetry, then we get the situation illustrated in Fig. 16.2(b), where the twofold degeneracy remains.

However, if there is no inversion symmetry, then the only relationships that remain are those of (16.23) and (16.24) shown in Fig. 16.2(c), and the Kramers degeneracy results in $E_\uparrow(\boldsymbol{k}) = E_\downarrow(-\boldsymbol{k})$ and $E_\downarrow(\boldsymbol{k}) = E_\uparrow(-\boldsymbol{k})$.

The role of inversion symmetry is also important for the $E(\boldsymbol{k})$ relations for degenerate bands. This is illustrated in Fig. 16.3 for degenerate bands near $\boldsymbol{k} = 0$. We take as examples: (a) diamond for which the spin–orbit interaction can be neglected and all levels are doubly degenerate at a general point in the Brillouin zone, (c) InSb or GaAs which have T_d symmetry (lacking inversion) so that relations (16.23) and (16.24) apply and the twofold Kramers degeneracy is lifted by the Dresselhaus-spin–orbit term [25], (b) Ge or Si which have O_h symmetry (including inversion) and the twofold Kramers degeneracy is retained at a general point in the Brillouin zone.

We give in Table 16.2 the general Herring rules (see Sect. 16.3) which apply whether or not the spin–orbit interaction is included. When the spin–orbit interaction is included, there are also three cases which can be distinguished. When the time reversal operator $\hat{T}$ acts on a spin dependent wavefunction ψ

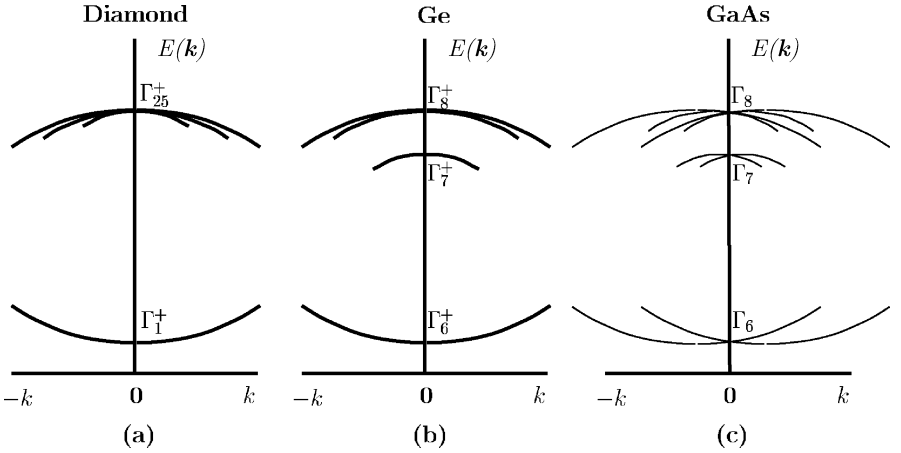

Fig. 16.3. Schematic examples of energy bands $E(\boldsymbol{k})$ near $\boldsymbol{k} = 0$: (a) in diamond without spin-orbit interaction, each band having a twofold spin degeneracy. (b) in Ge where the spin-orbit interaction split bands, with each band remaining at least doubly degenerate. (c) in GaAs where the Γ_8 bands are split by the spin-orbit interaction and the degeneracy occurs only at $\boldsymbol{k} = 0$. At a general $\boldsymbol{k}$ point the levels do not stick together. The magnitudes of the splittings are not to scale

Table 16.2. Summary of Herring rules regarding degeneracies and time reversal

case	relation between D and D^*	Frobenius–Schur test	spinless electron	half-integral spin electron
(a)	D and D^* are equivalent to the same real irreducible representation	$\sum_R \chi(Q_0^2) = h$	no extra degeneracy	doubled degeneracy
(b)	D and D^* are inequivalent	$\sum_R \chi(Q_0^2) = 0$	doubled degeneracy	doubled degeneracy
(c)	D and D^* are equivalent to each other but not to a real representation	$\sum_R \chi(Q_0^2) = -h$	double degeneracy	no extra degeneracy

which transforms according to an irreducible representation D, then we have three possibilities:

(a) If the representation D is real, or can be transformed by a unitary transformation into a set of real matrices, then the action of $\hat{T}$ on these matrices will yield the same set of matrices. To achieve the required additional degeneracy, we must have D occur twice.
(b) If representations D and D^* cannot be brought into equivalence by a unitary transformation, then the corresponding levels must stick together in pairs to satisfy the time reversal degeneracy requirement.

Table 16.3. Character table for the double group C_4[a]

C_4	E	$\bar{E}$	C_4	$\bar{C}_4$	C_2	$\bar{C}_2$	C_4^{-1}	$\bar{C}_4^{-1}$	time inv.	basis for group C_4
Γ_1	1	1	1	1	1	1	1	1	a	z or S_z
Γ_2	1	1	-1	-1	1	1	-1	-1	a	xy
Γ_3	1	1	i	i	-1	-1	$-i$	$-i$	b	$-i(x+\mathrm{i}y)$ or $-(S_x+\mathrm{i}S_y)$
Γ_4	1	1	$-i$	$-i$	-1	-1	i	i	b	$i(x-\mathrm{i}y)$ or $(S_x-\mathrm{i}S_y)$
Γ_5	1	-1	ω	$-\omega$	i	$-i$	$-\omega^3$	ω^3	b	$\phi(1/2,1/2)$
Γ_6	1	-1	$-\omega^3$	ω^3	$-i$	i	ω	$-\omega$	b	$\phi(1/2,-1/2)$
Γ_7	1	-1	$-\omega$	ω	i	$-i$	ω^3	$-\omega^3$	b	$\phi(3/2,-3/2)$
Γ_8	1	-1	ω^3	$-\omega^3$	$-i$	i	$-\omega$	ω	b	$\phi(3/2,3/2)$

[a] In the table $i = \mathrm{e}^{\mathrm{i}\pi/2}$ and $\omega = \mathrm{e}^{\mathrm{i}\pi/4}$, and $\bar{E}$, $\bar{C}_4$, $\bar{C}_2$ and $\bar{C}_4^{-1}$ denote $\mathcal{R}E$, $\mathcal{R}C_4$, $\mathcal{R}C_2$ and $\mathcal{R}C_4^{-1}$ where $\mathcal{R}$ is rotation by 2π (see Chap. 14)

(c) If representations D and D^* can be brought into equivalence but neither can be made all real, then no additional degeneracy need be introduced and both make up the time reversal degenerate pair.

These results are summarized in Table 16.2 for both the case of no spin and when spin–orbit interaction is included. We now illustrate these rules with two cases:

(i) The double group representations of point group C_4 (symmorphic);
(ii) The double group representation at the L point in Ge (or Si) where the levels are degenerate by time reversal symmetry (nonsymmorphic).

For the first illustration, we give in Table 16.3 the character table for the double group C_4 discussed in the literature [47, 48]. We note that the double group tables contain an entry for time inversion, which summarizes the results discussed in Sect. 16.1 for the spinless bands. Inspection of this character table shows that the double group representations involve the 4th roots of unity (as shown below) and obey the relation $\chi(A_i) = -\chi(\bar{A}_i)$ for each of the pairs of symmetry operations A_i and $\bar{A}_i$ where $\bar{A}_i = \mathcal{R}A_i$. Note that the character table originally given in Koster has some misprints with regard to $\chi(C_4^{-1}) = -\chi(\bar{C}_4^{-1})$, which are corrected in Table 16.3. Table 16.4 clearly shows that the characters for the Γ_5 and Γ_6 irreducible representations are time reversal degenerate pairs, and likewise for the Γ_7 and Γ_8 irreducible representations.

For the double group representations, we consider the character $\chi(Q_0\bar{Q}_0)$ in applying the Herring rules which is also known in the literature as the Frobenius–Schur test. Application of the Frobenius–Schur test for Γ_5 gives

Table 16.4. Characters for Γ_5, Γ_6, Γ_7 and Γ_8 irreducible representations in terms of $\omega = \mathrm{e}^{\mathrm{i}\pi/4}$

	E	$\bar{E}$	C_4	$\bar{C}_4$	C_2	$\bar{C}_2$	C_4^{-1}	$\bar{C}_4^{-1}$
Γ_5:	ω^0	ω^4	ω	ω^5	ω^2	ω^6	ω^7	ω^3
Γ_6:	ω^0	ω^4	ω^7	ω^3	ω^6	ω^2	ω	ω^5
Γ_7:	ω^0	ω^4	ω^5	ω	ω^2	ω^6	ω^3	ω^7
Γ_8:	ω^0	ω^4	ω^3	ω^7	ω^6	ω^2	ω^5	ω

$$\sum \chi(Q_0\bar{Q}_0) = (1)(-1) + (1)(-1) - \omega^2 - \omega^2 + 1 + 1 - \omega^6 - \omega^6$$
$$= -1 - 1 - i - i + 1 + 1 + i + i = 0\,, \tag{16.29}$$

and shows that Γ_5 is type "b" under time reversal symmetry. By doing a similar Frobenius–Schur test for the other double group irreducible representations of double group C_4 we find that the representations Γ_6, Γ_7 and Γ_8 are also of the b type with respect to time reversal symmetry and this information is also given in Table 16.3.

For the second illustration involving the L-point levels in Ge, see the $E(\boldsymbol{k})$ diagram in Fig. 14.1(b) for the case where the spin–orbit interaction is included. The character table appropriate to the L-point (group D_{3d}) is given in Table 16.5. The character table for the group of the wave vector for the L point for the diamond structure is given in Table C.18 in the absence of spin. Since the translation $\boldsymbol{\tau}_d = (a/4)(1,1,1)$ does not enter into any of the symmetry operations, the classes can be simply represented as in Table 16.5.

The designations for the L-point representations have been added on the left column of Koster's table which is given in general in Table 16.5 for a double group for D_{3d} symmetry. This example shows the importance of checking the notation used in the literature for dispersion relations (Fig. 14.1(b)) and the notation used in general tables for double groups (Table 16.5) to verify that they are internally consistent.

For a Λ point (group D_3), the operations $E, 2C_3$ and $3C_2'$ take $\boldsymbol{k} \to -\boldsymbol{k}$ so each symmetry operation corresponds to an operator of the Q_0 type. For the L-point (group D_{3d}) also, all operations are of the Q_0 type, so that for the representations L_1, L_2 and L_3, we have $\Sigma\chi(Q_0\bar{Q}_0) = 12$, yielding representations of type a, in agreement with the character table for D_{3d} (Table 16.5). For the double group representation L_6^+ we obtain

$$L_6^+ = \Sigma\chi(Q_0\bar{Q}_0) = -4 - 2 + 0 - 4 - 2 + 0 = -12 \quad \text{type } (c)\,, \tag{16.30}$$

where again we write $Q_0\bar{Q}_0$ or $Q_0\mathcal{R}Q_0$ for Q_0^2. For the double group representation L_4^+, the Frobenius–Schur test yields

$$L_4^+ : \Sigma\chi(Q_0\bar{Q}_0)) = -1 - 2 + 3 - 1 - 2 + 3 = 0 \quad \text{type } (b)\,. \tag{16.31}$$

Table 16.5. Character table and basis functions for the double group D_{3d} [48]

D_{3d}	E	$\bar{E}$	$2C_3$	$2\bar{C}_2$	$3C_2'$	$3\bar{C}_2'$	I	$\bar{I}$	$2S_6$	$2\bar{S}_6$	$3\sigma_d$	$3\bar{\sigma}_d$	time inv.	bases
L_1^+ Γ_1^+	1	1	1	1	1	1	1	1	1	1	1	1	a	R
L_2^+ Γ_2^+	1	1	1	1	−1	−1	1	1	1	1	−1	−1	a	S_x
L_3^+ Γ_3^+	2	2	−1	−1	0	0	2	2	−1	−1	0	0	a	$(S_x - \mathrm{i}S_y)$, $-(S_x + \mathrm{i}S_y)$
L_1^- Γ_1^-	1	1	1	1	1	1	−1	−1	−1	−1	−1	−1	a	zS_z
L_2^- Γ_2^-	1	1	1	1	−1	−1	−1	−1	−1	−1	1	1	a	z
L_3^- Γ_3^-	2	2	−1	−1	0	0	−2	−2	1	1	0	0	a	$(x - \mathrm{i}y)$, $-(x + \mathrm{i}y)$
L_6^+ Γ_4^+	2	−2	1	−1	0	0	2	−2	1	−1	0	0	c	$\phi(1/2, -1/2)$
L_4^+ Γ_5^+	1	−1	−1	1	i	$-i$	1	−1	−1	1	i	$-i$	b	$\phi(3/2, -3/2)$ $-\mathrm{i}\phi(3/2, 3/2)$
L_5^+ Γ_6^+	1	−1	−1	1	$-i$	i	1	−1	−1	1	$-i$	i	b	$-(\phi(3/2, 3/2)$ $-\mathrm{i}\phi(3/2, -3/2))$
L_6^- Γ_4^-	2	−2	1	−1	0	0	−2	2	−1	1	0	0	c	$\Gamma_4^+ \times \Gamma_1^-$
L_4^- Γ_5^-	1	−1	−1	1	i	$-i$	−1	1	1	−1	$-i$	i	b	$\Gamma_5^+ \times \Gamma_1^-$
L_5^- Γ_6^-	1	−1	−1	1	$-i$	i	−1	1	1	−1	i	$-i$	b	$\Gamma_6^+ \times \Gamma_1^-$

Likewise L_5^+ is of type b. Since L_4^+ and L_5^+ are complex conjugate representations, L_4^+ and L_5^+ form time reversal degenerate pairs. Similarly, L_4^- and L_5^- are type b representations and form time reversal degenerate pairs (see Figs. 14.1(b) and 16.2(b)). For both L_4^+ and L_5^+ (and likewise for L_4^- and L_5^-) which are type (b) under time reversal symmetry, the dispersion shown in Fig. 16.2(b) applies. To obtain the regime shown in Fig. 16.2(c), the crystal should have no spatial inversion symmetry, which is pertinent to the zinc blende structure. Finally in Table 16.5 we see basis function entries of the form $\phi(1/2, -1/2)$ which denote spherical harmonics for which the two entries $1/2$ and $-1/2$, respectively, denote $j = 1/2$ and $m_j = -1/2$.

With this discussion of time reversal symmetry, we have explained all the entries to the character tables, and have explained why because of time reversal symmetry certain bands stick together on the $E(\boldsymbol{k})$ diagrams, such as in Fig. 14.1(b).

16.5 Magnetic Groups

If atoms at each lattice site can be represented as a charge distribution $\rho(\boldsymbol{r})$ with no particular spin symmetry (paramagnetic or diamagnetic), the ordi-

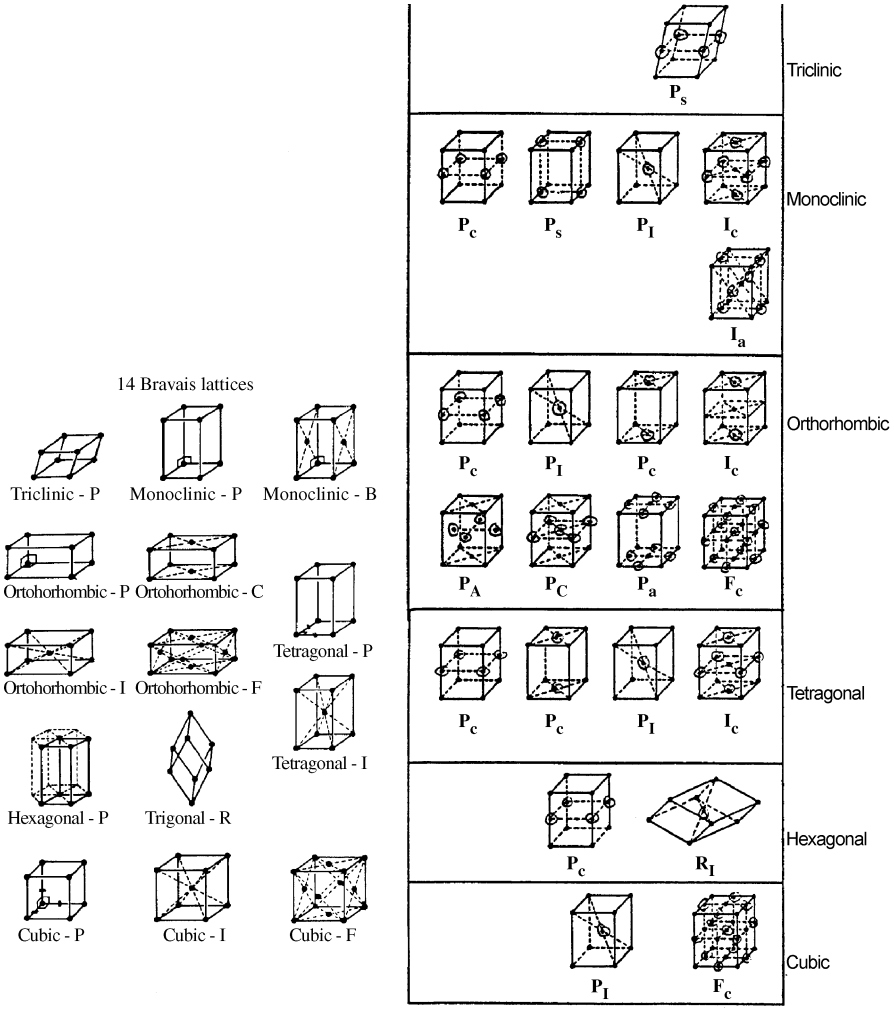

Fig. 16.4. (**a**) The 14 ordinary Bravais lattices on the *left* and (**b**) the 22 additional magnetic Bravais lattices on the *right*. The *open circles* represent the time reversed sites

nary space groups are used. If, however, we have ordered arrangements of spins, then the time reversal operator (which reverses the spin direction) can be combined with other group elements to form elements of a new type of symmetry group. Groups in which the time reversal operator forms group elements are called *magnetic space groups* and the corresponding point groups are called *magnetic point groups*. In this section we present some of the essential properties of magnetic space groups and give some examples of interest to solid state physics [54, 70].

16.5.1 Introduction

When magnetically ordered phases are taken into account, the magnetic unit cell is often larger than the chemical unit cell, as for example in an antiferromagnetic system. Additional symmetry elements are introduced (see Sect. 16.5.2), and as a result many more point groups and space groups are possible (see Sect. 16.5.3).

There are, in fact, **122** $(58 + 2 \times 32)$ magnetic point groups (rather than 32), and **1,651** $(1,191+2\times230)$ magnetic space groups (rather than 230), and 36 $(22 + 14)$ magnetic Bravais lattices rather than 14. The magnetic Bravais lattices which are important for describing antiferromagnetic structures are shown in Fig. 16.4(b), and for comparison the 14 ordinary Bravais lattices are also shown in Fig. 16.4(a), and are further explained below. We will confine our brief discussion to magnetic single groups (not double groups) and we shall only discuss magnetic point groups, and showing their connection to time reversal symmetry.

16.5.2 Types of Elements

Magnetic groups have symmetry elements corresponding to unitary operators (denoted by A_i) and antielements $M_k = \hat{T}A_k$ corresponding to antiunitary operators, where $\hat{T}$ is the antiunitary time reversal operator (see Sect. 16.2). We show in Fig. 16.5(a) a one-dimensional lattice in which $\hat{T}$ when combined with a translation is a symmetry operation. However, by displacing the nonmagnetic white atoms relative to the magnetic shaded atoms in Fig. 16.5(b) relative to their positions in Fig. 16.5(a), we see that $\hat{T}$ is no longer a symmetry operation. The lowering of the symmetry of the chain of atoms introduced by the spin on the magnetic ion breaks the time reversal symmetry in Fig. 16.5(b) as the spin-up magnetic species attracts the nonmagnetic ion relative to the interaction with the spin-down magnetic ion. This structural

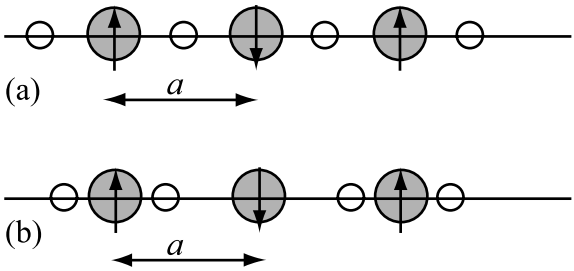

Fig. 16.5. Diagram showing a one-dimensional lattice where the white atoms are nonmagnetic and the shaded atoms are magnetic with the indicated direction of spin angular momentum: (**a**) the operation $\hat{T}$ is combined with translation as a space group symmetry operation, (**b**) $\hat{T}$ is not a symmetry operation of the group, even if combined with translations

lattice distortion represents another manifestation of the Jahn–Teller effect (see Sect. 7.7).

The product of two unitary elements A_i or of two antiunitary elements M_k yields a unitary element, while the product of a unitary element A_i with an antiunitary element M_k yields an antiunitary element:

$$\begin{aligned} A_i A_{i'} &= A_{i''} \\ A_i M_k &= M_{k'} \\ M_k A_i &= M_{k''} \\ M_k M_{k'''} &= A_{i'''} \,. \end{aligned} \tag{16.32}$$

To satisfy these relations, group properties and the rearrangement theorem, there must be *equal numbers* of elements of the type A_i and of the type M_k in a magnetic point group.

16.5.3 Types of Magnetic Point Groups

In classifying the magnetic point groups we must consider three types of point groups:

(a) 32 ordinary point groups G' where $\hat{T}$ is not an element.
(b) 32 ordinary point groups $G' \otimes \hat{T}$. In these magnetic point groups, all elements A_i of G' are contained together with all elements $\hat{T}A_i$.
(c) 58 point groups G in which half of the elements are $\{A_i\}$ and half are $\{M_k\}$ where $M_k = \hat{T}A_k$ and the $\{A_i, A_k\}$ form an ordinary point group G'. Also $\{A_i\}$ is a subgroup of G'. It is important to emphasize that the M_k elements are made from A_k elements that are different from the A_i elements.

Summing the number of types (a), (b), and (c) we obtain $(32+32+58) = 122$ magnetic point groups. Case (a) can apply to nonmagnetic materials and some ferromagnetic materials. Case (b) can apply to some antiferromagnetic materials. Case (c) can apply to magnetic materials with a variety of spin orderings.

We list in Table 16.6 the 58 magnetic point groups of type (c) and denoted by G; also included in the table are the 32 ordinary point groups of type (a) which are denoted by G' [70]. The 32 point groups of type (b), obtained from those in type (a) as $G' \otimes \hat{T}$, are not listed. The magnetic groups of type (c) are related to elements of a group G' and a subgroup H_r and are denoted by $G'(H_r)$. The appropriate group G' contains the symmetry elements $\{A_i, A_k\}$ while the subgroup H_r of G' only has elements $\{A_i\}$.

16.5.4 Properties of the 58 Magnetic Point Groups $\{A_i, M_k\}$

We list below some of the properties of the magnetic point groups [type (c)] that contain both unitary and antiunitary symmetry elements, A_i and $M_k =$

Table 16.6. The magnetic point groups of type (a) and type (c)

crystal system	*group G'*	*number of elements*	*invariant unitary subgroup H*	*Shubnikov notation*	*international notation*	*magnetic order*
triclinic	C_1	1	C_1	$\underline{1}$	$\underline{1}$	F
	$S_2(C_i)$	2	S_2	$\underline{\bar{2}}$	$\underline{\bar{1}}$	F
			C_1	$\underline{2}$	$\underline{1}$	AF
monoclinic	C_{1h}	2	C_{1h}	m	m	F
			C_1	$\underline{m}$	$\underline{m}$	F
	C_2	2	C_2	2	2	F
			C_1	$\underline{2}$	$\underline{2}$	F
	C_{2h}	4	C_{2h}	$2{:}m$	$2/m$	F
			C_i	$2{:}\underline{m}$	$2/\underline{m}$	F
			C_2	$2{:}\underline{m}$	$2/\underline{m}$	AF
			C_{1h}	$\underline{2}{:}m$	$\underline{2}/m$	AF
rhombic	C_{2v}	4	C_{2v}	$2{\cdot}m$	$2mm$	AF
			C_{1h}	$\underline{2}{\cdot}m$	$\underline{2m}m$	F
			C_2	$2{\cdot}\underline{m}$	$2\underline{mm}$	F
	D_2	4	D_2	$2{:}2$	222	AF
			C_2	$2{:}\underline{2}$	$2\underline{22}$	F
	D_{2h}	8	D_{2h}	$m{\cdot}2{:}m$	mmm	AF
			C_{2h}	$\underline{m}{\cdot}2{:}m$	$\underline{mm}m$	F
			C_{2v}	$m{\cdot}2{:}\underline{m}$	$mm\underline{m}$	AF
			D_2	$\underline{m}{\cdot}2{:}\underline{m}$	$\underline{mm}\underline{m}$	AF
tetragonal	C_4	4	C_4	4	4	F
			C_2	$\underline{4}$	$\underline{4}$	AF
	S_4	4	S_4	$\bar{4}$	$\bar{4}$	F
			C_2	$\underline{\bar{4}}$	$\underline{\bar{4}}$	AF
	C_{4h}	8	C_{4h}	$4{:}m$	$4/m$	F
			C_{2h}	$\underline{4}{:}m$	$\underline{4}/m$	AF
			C_4	$4{:}\underline{m}$	$4/\underline{m}$	AF
			S_4	$\underline{4}{\cdot}\underline{m}$	$\underline{4}/\underline{m}$	AF
	D_{2d}	8	D_{2d}	$\bar{4}{\cdot}m$	$\bar{4}2m$	AF
			C_{2v}	$\underline{\bar{4}}{\cdot}m$	$\underline{\bar{4}}2m$	AF
			D_2	$\bar{4}{\cdot}\underline{m}$	$\bar{4}2\underline{m}$	AF
			S_4	$\bar{4}{\cdot}\underline{m}$	$\bar{4}2\underline{m}$	F
	C_{4v}	8	C_{4v}	$4{\cdot}m$	$4mm$	AF
			C_{2v}	$\underline{4}{\cdot}m$	$\underline{4m}m$	AF
			C_4	$4{\cdot}\underline{m}$	$4\underline{mm}$	F
	D_4	8	D_4	$4{:}2$	$42(422)$	AF
			D_2	$\underline{4}{:}2$	$\underline{42}$	AF
			C_4	$4{:}\underline{2}$	$4\underline{2}$	F
	D_{4h}	16	D_{4h}	$m{\cdot}4{:}m$	$4/mmm$	AF
			D_{2h}	$m{\cdot}\underline{4}{:}m$	$4/m\underline{mm}$	AF
			C_{4h}	$\underline{m}{\cdot}4{:}m$	$4/\underline{m}mm$	F
			D_{2d}	$m{\cdot}\underline{4}{:}\underline{m}$	$\underline{4}/m\underline{m}\underline{m}$	AF
			C_{4v}	$m{\cdot}4{:}\underline{m}$	$4/\underline{m}mm$	AF
			D_4	$\underline{m}{\cdot}4{:}\underline{m}$	$4/\underline{mmm}$	AF

(Group G' is a point group and the underscores on the Shubnikov notation denote elements of G' to which $\hat{T}$ has been adjoined. F and AF denote ferromagnetic and antiferromagnetic ordering, respectively)

Table 16.6. (continued)

crystal system	*group G'*	*number of elements*	*invariant unitary subgroup H*	*Shubnikov notation*	*international notation*	*magnetic order*
rhombohedral	C_3	3	C_3	3	3	F
	S_6	6	S_6	$\bar{6}$	$\bar{3}$	F
			C_3	$\underline{\bar{6}}$	$\underline{\bar{3}}$	AF
	C_{3v}	6	C_{3v}	$3\cdot m$	$3m$	AF
			C_3	$3\cdot\underline{m}$	$3\underline{m}$	F
	D_3	6	D_3	$3{:}2$	32	AF
			C_3	$3{:}\underline{2}$	$3\underline{2}$	F
	D_{3d}	12	D_{3d}	$\bar{6}\cdot m$	$\bar{3}m$	AF
			S_6	$\bar{6}\cdot\underline{m}$	$\bar{3}\underline{m}$	F
			C_{3v}	$\underline{\bar{6}}\cdot m$	$\underline{\bar{3}}m$	AF
			D_3	$\underline{\bar{6}}\cdot\underline{m}$	$\underline{\bar{3}}\underline{m}$	AF
hexagonal	C_{3h}	6	C_{3h}	$3{:}m$	$\bar{6}$	F
			C_3	$3{:}\underline{m}$	$\underline{\bar{6}}$	AF
	C_6	6	C_6	6	6	F
			C_3	$\underline{6}$	$\underline{6}$	AF
	C_{6h}	12	C_{6h}	$6{:}m$	$6/m$	F
			S_6	$\underline{6}{:}\underline{m}$	$\underline{6}/\underline{m}$	AF
			C_{3h}	$\underline{6}{:}m$	$\underline{6}/m$	AF
			C_6	$6{:}\underline{m}$	$6/\underline{m}$	AF
	D_{3h}	12	D_{3h}	$m\cdot 3{:}m$	$\bar{6}m2$	AF
			C_{3v}	$m\cdot 3{:}\underline{m}$	$\underline{\bar{6}}m2$	AF
			D_3	$\underline{m}\cdot 3{:}\underline{m}$	$\underline{\bar{6}}\underline{m}2$	AF
			C_{3h}	$\underline{m}\cdot 3{:}m$	$\underline{\bar{6}}m2$	F
	C_{6v}	12	C_{6h}	$6\cdot m$	$6mm$	AF
			C_{3v}	$\underline{6}\cdot m$	$\underline{6}m\underline{m}$	AF
			C_6	$6\cdot\underline{m}$	$6m\underline{m}$	F
	D_6	12	D_6	$6{:}2$	$62(622)$	AF
			D_3	$\underline{6}{:}2$	$\underline{6}2$	AF
			C_6	$6{:}\underline{2}$	$6\underline{2}$	F
	D_{6h}	24	D_{6h}	$m\cdot 6{:}m$	$6/mmm$	AF
			D_{3d}	$m\cdot\underline{6}{:}\underline{m}$	$6/m\underline{m}m$	AF
			C_{6h}	$\underline{m}\cdot 6{:}m$	$6/m\underline{m}\underline{m}$	F
			D_{3h}	$m\cdot\underline{6}{:}m$	$\underline{6}/m\underline{m}m$	AF
			C_{6v}	$m\cdot 6{:}\underline{m}$	$6/\underline{m}mm$	AF
			D_6	$\underline{m}\cdot 6{:}\underline{m}$	$6/\underline{m}m\underline{m}$	AF
cubic	T	12	T	$3/2$	23	AF
	T_h	24	T_h	$\bar{6}/2$	$m3$	AF
			T	$\underline{\bar{6}}/2$	$\underline{m}3$	AF
	T_d	24	T_d	$3/\bar{4}$	$\bar{4}3m$	AF
			T	$3/\underline{\bar{4}}$	$\underline{\bar{4}}3\underline{m}$	AF
	O	24	O	$3/4$	$43(432)$	AF
			T	$3/\underline{4}$	$\underline{4}3$	AF
	O_h	48	O_h	$\bar{6}/4$	$m3m$	AF
			T_h	$\bar{6}/4$	$m3\underline{m}$	AF
			T_d	$\underline{\bar{6}}/\underline{4}$	$\underline{m}3m$	AF
			O	$\underline{\bar{6}}/4$	$\underline{m}3\underline{m}$	AF

$\hat{T}A_k$, respectively. We denote a typical magnetic point group of this category by $G = \{A_i, M_k\}$.

(a) $\hat{T}$ is not an element in the magnetic point group G (since the identity element is one of the elements of $\{A_i\}$ but not of $\{A_k\}$).
(b) A_i and A_k are distinct, so that no element in the set $\{A_i\}$ is also in $\{A_k\}$ where $\{M_k\} = \{\hat{T}A_k\}$. If there were one A_j in common, then we could have $\hat{T}A_j$ in $\{M_k\}$ and A_j^{-1} in $\{A_i\}$, which on multiplication $\hat{T}A_jA_j^{-1}$ implies that $\hat{T}$ is in G, in contradiction with property (a).
(c) $G' \equiv \{A_i, A_k\}$ is one of the 32 ordinary point groups.
(d) The set $H_r = \{A_i\}$ forms an invariant unitary subgroup of G. This subgroup is selfconjugate because conjugation of an element in A_i with any element in $\{M_k\}$ written as $M_kA_iM_k^{-1}$ yields an element in $\{A_i\}$ as a result of (16.32), and likewise the conjugation $A_iM_kA_i^{-1}$ yields an element in $\{M_k\}$.
(e) The number of unitary operators A_i = the number of antiunitary operators M_k, to satisfy the multiplication rules in (16.32) and the group properties of G.
(f) $\{A_i\}$ is the only coset of H_r in G and $\{A_k\}$ is the only coset of H_r in G'.
(g) Since H_r and G' are groups, and properties (e) and (f) apply, then G is a group of the form

$$G = H_r + \hat{T}(G' - H_r)\,. \tag{16.33}$$

(h) From property (g), we see that the procedure for finding magnetic point groups is to start with one of the 32 point groups G' and find all invariant subgroups H_r of *index 2* where half of the elements in G' are in H_r and half are not. Denoting each such subgroup by H_r we can form a magnetic group G_r such that

$$G_r = H_r + \hat{T}(G' - H_r)\,. \tag{16.34}$$

We denote each magnetic group G_r thus formed by $G'(H_r)$ in which the relevant G' and H_r for each G_r are listed. This notation is used in Table 16.6 and the various $G'(H_r)$ can be found in this table.

To illustrate the elements of magnetic point groups, we consider the four entries under C_{2h} in Table 16.6. We then list below the symmetry elements of each of the $C_{2h}(H_r)$ magnetic point groups.

$$\begin{aligned}
C_{2h}(C_{2h}): &\quad E, C_2, i, iC_2\,, \quad (iC_2 = \sigma_h)\\
C_{2h}(C_2): &\quad E, C_2, \hat{T}i, \hat{T}iC_2\\
C_{2h}(C_i): &\quad E, i, \hat{T}C_2, \hat{T}iC_2\\
C_{2h}(C_{1h}): &\quad E, iC_2, \hat{T}i, \hat{T}C_2\,,
\end{aligned} \tag{16.35}$$

in which the magnetic point group $C_{2h}(C_{2h})$ is of type (a), and the other three are of type (c). Not listed is the magnetic space group $C_{2h} \otimes \hat{T}$ of type (b) which contains the eight symmetry elements $\{A_i\} = \{E, C_2, i, iC_2\}$ and

$\{\hat{T}\otimes A_i\} = \{\hat{T}, \hat{T}C_2, \hat{T}i, \hat{T}iC_2\}$ (see Table A.6 in Appendix A for the character table for C_{2h}). We note that the time reversal operator of $\hat{T}$ reverses the sign of a spin, while the *inversion operator i leaves a spin invariant* (since the angular momentum $\boldsymbol{L}$ is even under inversion, while $\boldsymbol{r}$ and $\boldsymbol{p}$ are each odd).

16.5.5 Examples of Magnetic Structures

We give below three examples of magnetic structures in each case illustrating a different aspect of magnetic structures. First we illustrate an orthorhombic ferromagnetic structure for which the magnetic unit cell and the chemical unit cell are the same (see Fig. 16.6).

The symmetry of this magnetic structure is denoted by D_{2h} (C_{2h}) which denotes a point group D_{2h} from which the subgroup (C_{2h}) forms the set of symmetry elements $\{A_i\}$ and the remaining symmetry elements of G' are $\{A_k\}$ where the elements M_k in G are of the form $M_k = \hat{T}A_k$. We note from Table 16.6 that D_{2h} (C_{2h}) corresponds to a ferromagnetic structure such as the one shown in Fig. 16.6. In the paramagnetic state, the proper symmetry group for this structure in D_{2h}.

The symmetry operations for $D_{2h} = D_2 \otimes i$ are E, C_{2x}, C_{2y}, C_{2z}, i, iC_{2x}, iC_{2y}, iC_{2z} [see Appendix A for character tables for D_{2h} (Table A.7) and C_{2h} (Table A.6)]. It is immediately seen that the subgroup of D_{2h} which leaves the spin invariant consists of the elements $\{A_i\} = E$, C_{2z}, i, iC_{2z}, since both orbital and spin angular momentum are invariant under inversion. These four elements form the group $C_{2h} = C_2 \otimes i$, noting again that the spin angular momentum S is even under inversion. The remaining elements of D_{2h} reverse the spins, so that the time reversal operator $\hat{T}$ is needed to keep all the spins

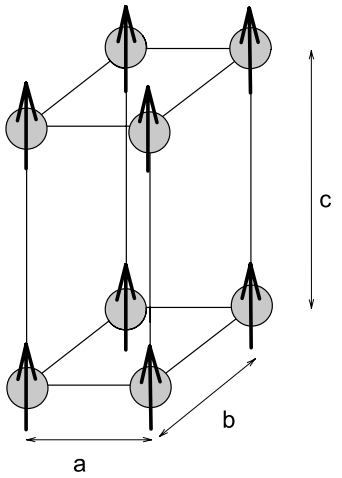

Fig. 16.6. Magnetic spin arrangement in $D_{2h}(C_{2h})$ symmetry for an orthorhombic ferromagnetic system

ferro-magnetically aligned. We therefore obtain $\{M_k\} = \hat{T}C_{2x}, \hat{T}C_{2y}, \hat{T}iC_{2x}$ and $\hat{T}iC_{2y}$ for the remaining symmetry elements of D_{2h} (C_{2h}). The appropriate Bravais lattice in this case is the orthorhombic-P Bravais lattice for the nonmagnetic groups (see Fig. 16.4(a)). The magnetic space group $D_{2h}(C_{2h})$ is further developed in Problem 16.5.

Next we consider for our second example antiferromagnets with the Rutile structure as shown in Fig. 16.7. The open circles are the F ions while the black circles with spins denote the magnetic cations. The point group for this structure in the paramagnetic state is $D_{4h} = D_4 \otimes i$. In the antiferromagnetic state, each unit cell has one spin up and one spin down cation. The chemical and magnetic unit cells contain the atoms shown in Fig. 16.7. The space group symmetry operations for D_{4h} pertinent to the rutile structure are the 16 operations listed below:

$$
\begin{aligned}
&1.\ \{E|0\} && 9.\ \{i|0\} && \\
&2.\ \{C_2|0\} && 10.\ \{\sigma_h|0\} && = \{C_2|0\}\{i|0\} \\
&3.\ \{C_{2\xi}|0\} && 11.\ \{\sigma_{d\xi}|0\} && = \{C_{2\xi}|0\}\{i|0\} \\
&4.\ \{C_{2\nu}|0\} && 12.\ \{\sigma_{d\nu}|0\} && = \{C_{2\nu}|0\}\{i|0\} \\
&5.\ \{C_4|\tau_0\} && 13.\ \{S_4^{-1}|\tau_0\} && = \{C_4|\tau_0\}\{i|0\} \\
&6.\ \{C_4^{-1}|\tau_0\} && 14.\ \{S_4|\tau_0\} && = \{C_4^{-1}|\tau_0\}\{i|0\} \\
&7.\ \{C_{2x}|\tau_0\} && 15.\ \{\sigma_{vx}|\tau_0\} && = \{C_{2x}|\tau_0\}\{i|0\} \\
&8.\ \{C_{2y}|\tau_0\} && 16.\ \{\sigma_{vy}|\tau_0\} && = \{C_{2y}|\tau_0\}\{i|0\}\,,
\end{aligned}
\tag{16.36}
$$

where the axes $\xi = (110)$ and $\nu = (1\bar{1}0)$ denote twofold axes and the translation $\boldsymbol{\tau}_0 = 1/2(\boldsymbol{a_1} + \boldsymbol{a_2} + \boldsymbol{a_3})$ is from the origin at the lower left hand corner of the figure to the body center of the unit cell (see Fig. 16.7). The point group

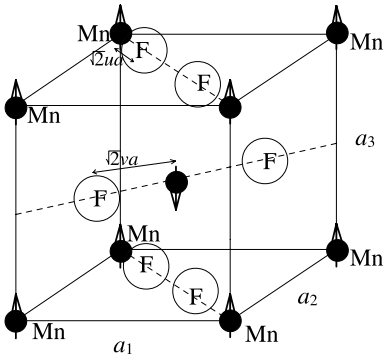

Fig. 16.7. Common antiferromagnets MnF_2, FeF_2 and CoF_2 crystallize in the rutile structure with $|a_1| = |a_2| = a$; $|a_3| = c$; $c \neq a$. The diagram emphasizes the magnetic unit cell for the rutile structure that has the magnetic point group D_{4h} (D_{2d}) which describes the antiferromagnetic spin alignment of these magnetic materials

D_{4h} corresponding to these space group operations is found by setting $\boldsymbol{\tau_0} = 0$. The character table for D_4 is given in Table A.18 where $D_{4h} = D_4 \otimes i$. The operations listed in (16.36) correspond to the space group for the chemical unit cell for the rutile structure.

The unitary subgroup that forms the symmetry group for antiferromagnetic MF_2 (M = magnetic cation) consists of the four elements of the symmetry group D_2 $\{E|0\}$, $\{C_2|0\}$, $\{C_{2x}|\tau_0\}$, $\{C_{2y}|\tau_0\}$ and four additional elements formed by combining these with inversion. These eight elements constitute $\{A_i\}$ which corresponds to the group $D_{2h} = D_2 \otimes i$ (see Table A.7). From Fig. 16.7 we see that the operations C_{2x} and C_{2y} invert the spins. The appropriate Bravais lattice for MnF_2 is the tetragonal Bravais lattice P_I for the magnetic groups (see Fig. 16.4). If we ignore the fluorine anions, the chemical unit cell would be half as large containing only one magnetic cation. The magnetic unit cell would then be twice as large as the chemical unit cell. Nevertheless the magnetic point group for the antiferromagnetic chemical structure remains D_{4h} (D_{2h}). Further elaboration on this space group is given in Problem 16.7.

As a third example we consider the magnetic states of EuSe because the nearest and next-nearest exchange constants are of approximately equal magnitude and of opposite sign, and for this reason EuSe exhibits several different and interesting magnetic phases, depending on the magnetic field and temperature variables. In Figs. 16.8(a)–(c) we see, respectively, the spin arrangement for the antiferromagnetic (AF-II) two spin (↑↓) phase, the ferri-

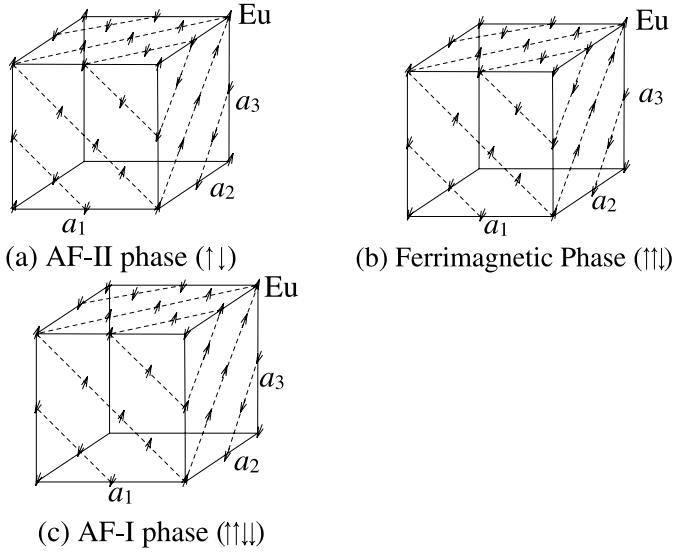

Fig. 16.8. Magnetic structure of EuSe in (**a**) the AF-II phase (↑↓), (**b**) the ferrimagnetic phase (↑↑↓), and (**c**) the antiferromagnetic AF-I phase (↑↑↓↓) in which the magnetic Eu spins are shown

magnetic three spin ($\uparrow\uparrow\downarrow$) phase, and the antiferromagnetic (AF-I) four spin ($\uparrow\uparrow\downarrow\downarrow$) phase.

A ferromagnetic phase is also found upon application of a high applied magnetic field. In all four magnetically ordered phases, the spins in a given $(1\bar{1}1)$ plane are parallel to each other and are oriented along the [011] direction. The resulting magnetic space group has very low symmetry. For the AF-II phase, the symmetry elements are $\{E|0\}$, $\{i|0\}$, $\hat{T}\{E|\boldsymbol{\tau_0}\}$, $\hat{T}\{i|\boldsymbol{\tau_0}\}$ in which the vector $\boldsymbol{\tau}_0$ takes the spins from one sublattice to the other

$$\boldsymbol{\tau}_0 = \frac{1}{4}(a_x, 0, a_z)\,. \tag{16.37}$$

Thus the magnetic point group is $S_2 \otimes \hat{T}$.

If, however, the spins were oriented instead along $[1\bar{1}1]$ and $[\bar{1}1\bar{1}]$ directions in alternate (111) planes, then the magnetic symmetry of the group increases and is $C_3 \otimes \hat{T}$. Thus the spin direction is important in determining the magnetic point group and the magnetic space group. We note that the number of sublattices (1, 2, 3, or 4) is also important in determining the symmetry operations in the magnetic space groups. For some cases it is useful to ignore the spin directions and just to consider each atom on a given sublattice as a colored atom. Such groups are called *color groups* [43]. Color groups have more symmetry than the magnetic groups.

16.5.6 Effect of Symmetry on the Spin Hamiltonian for the 32 Ordinary Point Groups

The n lowest energy states for electrons in a paramagnetic center where an external magnetic field H has been applied can be described by an Effective Spin Hamiltonian $\mathcal{H}_{\text{spin}}$ generally given by [59]:

$$\mathcal{H}_{\text{spin}} = \mathcal{H}_Z + \mathcal{H}_F + \mathcal{H}_{hf} + \mathcal{H}_{shf} + \mathcal{H}_{ZN} + \mathcal{H}_Q\,, \tag{16.38}$$

where the contributions from the electronic Zeeman effect $\mathcal{H}_Z$, the fine interaction $\mathcal{H}_F$, the hyper-fine interaction $\mathcal{H}_{hf}$, the super-hyper-fine interactions $\mathcal{H}_{shf}$, the nuclear Zeeman effect $\mathcal{H}_{ZN}$ and the nuclear quadrupole interaction $\mathcal{H}_Q$ are taken into account. Each of these contributions are represented by tensors, and the symmetries of the system can be used to evaluate the nonzero and the independent terms in $\mathcal{H}_{\text{spin}}$. The group theory procedure for dealing with general tensors is discussed in Chap. 18.

It is however interesting to comment here on the influence of symmetries in the spin Hamiltonian. If we limit ourselves to spin operators S transforming like angular momentum (invariant under spatial inversion and odd under time reversal symmetry), it is clear that different Hamiltonians related to each other by the spatial inversion are identical. Therefore, two groups obtained from each other by the direct multiplication with the inversion operator will indeed give the same $\mathcal{H}_{\text{spin}}$. They will be *magnetically equivalent.*

Table 16.7. Categories of magnetic equivalence for the 32 ordinary point groups

categories	1	2	3	4	5	6	7	8	9	10	11
	C_1	C_2	D_2	C_3	D_3	C_4	D_4	C_6	D_6	T	O
	S_2	C_{1h}	C_{2v}	S_6	C_{3v}	S_4	C_{4v}	C_{6h}	C_{6v}	T_h	T_d
		C_{2h}	D_{2h}		D_{3d}	C_{4h}	D_{2d}	C_{3h}	D_{3h}		O_h
							D_{4h}		D_{6h}		

Considering the 32 ordinary point groups, Table 16.7 gives the 11 categories of *magnetically equivalent* groups. It is enough to find $\mathcal{H}_{\text{spin}}$ for the lowest symmetry point groups for each of the 11 categories, and the spin Hamiltonian for the higher symmetry groups will be identical.

Selected Problems

16.1. Consider the space group D_{6h}^4 (#194) which we discussed in connection with the lattice modes for graphite (see Problem 11.1). We will now concern ourselves with the electronic structure of graphite. Since the Fermi surfaces are located close to the HK axes in the Brillouin zone, it is important to work with the group of the wave vector at points H, K and A (see Fig. 16.9).

(a) Using Appendix D and other literature references [47,54] give the character table including double groups for the group of the wave vector at point K. Classify each of the irreducible representations according to whether they behave as a, b or c under time reversal symmetry.
(a) Find the compatibility relations as we move away from K toward H.

16.2. Now consider a 2D graphene sheet, which by definition is one atomic layer of 3D graphite.

(a) What are the symmetry operations for this structure and what is the appropriate 2D space group?

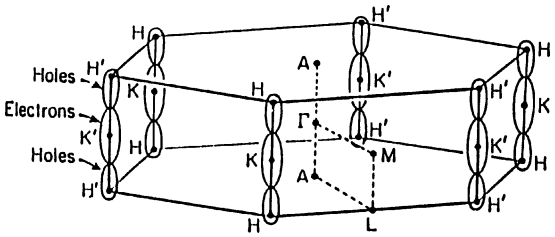

Fig. 16.9. Brillouin zone and Fermi surfaces for electrons and holes of semimetallic graphite

(b) Give the character table for the group of the wave vector at the Γ point (center of the Brillouin zone), and include the time reversal classification for the cases where the spin–orbit interaction is neglected and where it is included.
(c) Repeat part (b) for the group of the wave vector at the K point where the valence and conduction band are degenerate right at the K point (corner of the Brillouin zone) and have a linear k dependence as we move away from the K point. What is the relation between the K and K' points in the 2D Brillouin zone under time reversal symmetry? Consider the symmetry relation between $E_{\uparrow(k)}$ and $E_{\downarrow}(k)$ in the vicinity of the K and K' points for the linear k bands and for those coming into points K and K' with zero slope.

16.3. Consider the zinc blende space group (#227) which lacks inversion symmetry. For an energy band with two fold degeneracy, time reversal symmetry gives the relation $E(\boldsymbol{k}, \uparrow) = E(-\boldsymbol{k}, \downarrow))$ (see Sect. 16.4)

(a) What is the form of $E(\boldsymbol{k})$ as we move away from $\boldsymbol{k} = 0$?
(b) What is the form of the constant energy surface for the case where the carrier concentration is 10^{17} carriers/cm^3? Does time reversal symmetry have an effect on the constant energy surface at the Fermi level? What happens in the presence of a magnetic field for which $\mu^* B > E_{\mathrm{F}}$ and $\mu^* B < E_{\mathrm{F}}$?

16.4. Consider the symmetry operations of the arrangement of the chains of magnetic and nonmagnetic atoms in Fig. 16.5.

(a) What are the symmetry operations of the chain shown in Fig. 16.5(a)? What type of magnetic group would be applicable to the group of the wave vector for $k = 0$, using the classifications in Sect. 16.5.3.
(b) Repeat (a) for the case of the chain shown in Fig. 16.5(b). Fig. 16.5 for $E(k, \uparrow)$ under spatial and time inversion symmetry?

16.5. (a) For the ferromagnetic structure in Fig. 16.6, what is the difference between the chemical and magnetic unit cell [51]? What are the differences in the symmetry operations when the system is in the ferromagnetic state as compared to the paramagnetic states?
(b) What difference do you expect for $E(k)$ for the two cases in (a)? What is the effect of the time reversal operator on $E(k)$? Do you expect a change in $E(k)$ when a phase transition from a paramagnetic to a ferromagnetic state occurs?
(c) Suppose now that the spins were all aligned by a high magnetic field along the $\boldsymbol{a}$ axis. What would be the new magnetic group? On physical arguments, would you expect this to be a stable configuration when you turn off the magnetic field? Why? What information does group theory provide regarding this question?

16.6. Suppose that we have a magnetic compound MX (where M is the magnetic species) that crystallizes in the zinc-blende structure. Suppose that

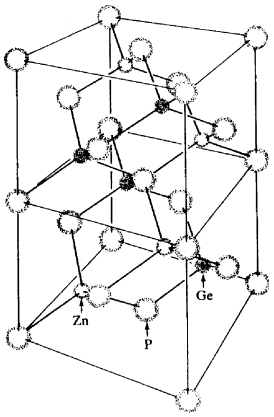

Fig. 16.10. In the chalcopyrite structure for $ZnGeP_2$, the lattice is compressed slightly along the vertical direction and the phosphorus atoms are slightly displaced from the positions they would have in the zinc blende structure

at the Neél temperature the magnetic species undergo a magnetic phase transition to an antiferromagnetic two sublattice phase such that by treating the M↑ and M↓ as different species, the magnetic crystal is described by the chalcopyrite structure (Fig. 16.10).

(a) Reconfigure the prototype chalcopyrite structure, shown in Fig. 16.10 for $ZnGeP_2$, to correspond to the antiferromagnetic MX compound with the two spin states. What is the space group for this structure?
(b) Find the change in the Raman spectra associated with this magnetic phase transition from the zinc-blende to the chalcopyrite structures shown in Fig. 16.10.

16.7. Consider the structure shown for MnF_2 in Fig. 16.7.

(a) What are the classes formed by the elements in (16.36)? What is the effect of time reversal symmetry on each of these classes?
(b) What is the appropriate space group for MnF_2 in the paramagnetic state? What changes occur at the magnetic phase transition to an antiferromagnetic state?
(c) The Raman effect probes certain lattice modes in this structure. Find the Raman active modes in the paramagnetic phase?
(d) What changes would you expect to see in the Raman spectra when the MnF_2 undergoes a magnetic phase transition to the magnetic $D_{4h}(D_{2d})$?

16.8. The ferrites (XFe_2O_4, X^{2+} = metallic ion) are important magnetic materials belonging to the cubic $Fd3m$ (O_h^7) space group. To calculate the spin Hamiltonian $\mathcal{H}_{\text{spin}}$ for this material, it is enough to obtain $\mathcal{H}_{\text{spin}}$ for one of the ordinary point groups of class 11 in Table 16.7. Show that the spin Hamiltonian can be written in the following form [3, 15, 34, 41]:

$$\mathcal{H}_{\text{spin}} = g\mu \boldsymbol{H}\cdot\boldsymbol{S} - g_N\mu_N \boldsymbol{H}\cdot\boldsymbol{I} + A\boldsymbol{I}\cdot\boldsymbol{S} + B_{40}(O_{40}+5O_{44}) + B_{60}(O_{60}+21O_{64})\,, \tag{16.39}$$

where

$$\begin{aligned}
O_{40} &= 35S_z^4 + 25S_z^3 - 30S(S+1)S_z^2 + 3S^2(S+1)^2 - 6S(S+1)\,,\\
O_{44} &= (1/2)(S_+^4 + S_-^4)\,,\\
O_{60} &= 231S_z^6 - 315S(S+1)S_z^4 + 735S_z^4 + 105S^2(S+1)^2S_z^2 - 525S(S+1)S_z^2\\
&\quad +294S_z^2 - 5S^3(S+1)^3 + 40S^2(S+1)^2 - 60S(S+1)\,,\\
O_{64} &= (1/2)(S_+^4 + S_-^4)(11S_z^2 - S(S+1) - 38)\,.
\end{aligned}$$